Lattice-BGK Approach to Simulating Granular Flows

M.-L. Tan,[1] Y. H. Qian,[1] I. Goldhirsch,[1, 2] and S. A. Orszag[1]

Many continuum theories for granular flow produce an equation of motion for the fluctuating kinetic energy density ("granular temperature") that accounts for the energy lost in inelastic collisions. Apart from the presence of an extra dissipative term, this equation is very similar in form to the usual temperature equation in hydrodynamics. It is shown how a lattice-kinetic model based on the Bhatnagar–Gross–Krook (BGK) equation that was previously derived for a miscible two-component fluid may be modified to model the continuum equations for granular flow. This is done by noting that the variable corresponding to the concentration of one species follows an equation that is essentially analogous to the granular temperature equation. A simulation of an unforced granular fluid using the modified model reproduces the phenomenon of "clustering instability," namely the spontaneous agglomeration of particles into dense clusters, which occurs generically in all granular flows. The success of the continuum theory in capturing the gross features of this basic phenomenon is discussed. Some shear flow simulations are also presented.

1. INTRODUCTION

The numerical solution of partial differential equations using methods based on the lattice-Bhatnagar–Gross–Krook (BGK[1]) models[27] offers a number of advantages over conventional computational methods. These include stable, efficient, and highly parallelizable algorithms, and the ease with which various rheological models and complex boundary conditions can be incorporated. Some of these advantages, such as stability and

---

[1] Fluid Dynamics Research Center, James Forrestal Campus, Princeton, New Jersey 08544-0710.

[2] Permanent Address: Department of Fluid Mechanics and Heat Transfer, Faculty of Engineering, Tel-Aviv University, Ramat Aviv, Tel-Aviv 69978, Israel.

87

parallelizability, are inherited from the lattice gas automata (LGA) models[6] first proposed for hydrodynamics in refs. 5 and 8, while others, such as noise-free dynamics, Galilean invariance, and a velocity-independent pressure, form the main thrusts of the LBGK models. These models are extremely versatile and can be applied to a variety of hydrodynamic phenomena including reaction–diffusion, phase transitions, magnetohydrodynamics, and multiphase flows.[29]

It is shown in this paper how an LBGK model can easily be adapted to solve continuum equations of motion for granular "fluids". The notion of a granular 'fluid' arises when a system of macroscopic grains, such as sand or coal particles, are subject to such rapid deformation rates that the contacts between individual grains do not endure and their motion is continuously randomized by frequent collisions. The behavior in this case is analogous to that of a classical fluid, with the difference that the collisions are inelastic. It is emphasized, however, that despite the analogy, granular fluids are rheologically very different from classical fluids. A most significant difference is the tendency of granular systems to form dense clusters of particles of low internal kinetic energy within a dilute ambient of energetic particles. These clusters have been observed in both externally driven and undriven systems (i.e., systems that are left to decay from initial energetic states). For example, anisotropic clusters are always found in sheared systems whose collisions are very inelastic.[32, 14, 34] Dense clusters can also be created spontaneously in an unforced and initially uniform system as its energy is dissipated in inelastic collisions.[11, 10, 22, 23, 21] Clustering formation has also been observed in chute flows,[25, 3] convection cells,[13] and fluidized beds and thus appear to be a generic feature of all granular flows.

Granular fluids have often been described constitutively on the basis of the classical kinetic theory of gases, and many theories of granular flow[24, 12, 18, 15, 16, 20, 19] produce continuum equations which include one for the kinetic energy density ("granular temperature") that accounts for the energy lost in inelastic collisions, in addition to the usual equations for the mass and momentum densities. These equations are very similar to those for elastic particles, differing only in the presence of an inelastic term in the kinetic energy equation. The important issue of how well they capture the basic phenomenology of granular flows has hitherto been addressed only in an indirect way, for example, by comparing the theoretical constitutive relation (i.e., the relationship between the stress and the strain rate) to data obtained in molecular dynamics simulations[2] or by performing stability analyses of simple flow configurations. Although much has been learnt from these comparisons and analyses, including the discovery that the stresses in the flow deviate significantly from their theoretical values in the

presence of "inelastic microstructure" and that typical flow configurations governed by the continuum equations are unstable with respect to density fluctuations[10, 30, 31] and typical length scales are deducible which characterize the distance between clusters,[10] it is still largely unclear whether many of the peculiar features of granular flows are captured at all by these equations. The neglect of higher order correlations among the particles in the derivation of the equations must already imply that they will not be faithful to the actual dynamics in dense regimes—and large density inhomogeneities are indeed commonplace in granular systems. Other features peculiar to granular systems that have been observed include anisotropic clustering, hysteresis effects, generalized phase transitions, non-trivial transients, and oscillations.[32] A direct numerical study of the continuum equations will therefore not only provide insights into the nature of these effects, but also expose the specific aspects of the actual granular flow not captured by the equations.

The rest of the paper is organized as follows: After a very brief review of the basic LBGK model, we show how it can be modified to simulate the dilute-limit form of the continuum equations for two-dimensional granular flow derived by Jenkins and Richman[17] (henceforth refered to as the JR equations). Then we compute some numerical solutions of these equations for both a freely decaying system and a sheared system. The solutions are compared to results obtained from the corresponding molecular dynamics simulations. Finally, some comments on the ability of the JR equations to capture the various phenomena in granular flows are given.

2. LBGK MODEL FOR GRANULAR FLOW

In the prototypical LBGK model, the following discrete analog of the BGK equation,

$$N_{pi}(\mathbf{x} + \mathbf{c}_{pi}, t+1) = N_{pi}(\mathbf{x}, t) - w[N_{pi}(\mathbf{x}, t) - N^e_{pi}(\mathbf{x}, t)] \qquad (1)$$

is solved on a regular lattice on which the set of particle densities $N_{pi}(x, t)$ are distributed. Here N_{pi} is the average density of particles with velocity $\mathbf{c}_{pi}$ (the indices p and i are explained below), t is the time, x is the position vector of a node on the lattice, and w is the relaxation parameter, which can be freely adjusted between 0 and 2. A generic choice for the equilibrium population $N^e_{pi}(\mathbf{x}, t)$ is

$$N^e_{pi} = t_p \rho \left[1 + \frac{c_{pi\alpha} u_\alpha}{c_s^2} + \frac{u_\alpha u_\beta}{2c_s^2} \left(\frac{c_{pi\alpha} c_{pi\beta}}{c_s^2} - \delta_{\alpha\beta} \right) \right] \qquad (2)$$

Here α and β are indices for the Cartesian components of the particle velocity (Greek letters shall henceforth denote the Cartesian components of a vector). The hydrodynamic velocity and density are u_α and ρ, respectively. The index p is equal to the square of the modulus of the particle velocity $c_{pi\alpha}$ and has been used to distinguish between velocities having different moduli. The index i denotes the different velocities in the same speed class p. The constant c_s is proportional to a weighted average of the $c_{pi\alpha}$ and is identified as the speed of sound in the model. Finally, t_p is a weighting factor, which depends on p and which is adjusted to obtain isotropic fourth-order tensor products of $c_{pi\alpha}$ and to ensure Galilean invariance of the dynamics. The choice (2) for the equilibrium population, when used together with (1), can be shown to lead to macrodynamic equations which, when truncated after the second order in u_α, are similar to the Navier–Stokes equations.[28]

An LBGK model for granular fluids can be adapted from a previously derived model for miscible fluids[29] by noting that in a two-species mixture the equation of motion for the concentration of one species is analogous to the equation for the granular temperature when a source and a sink of concentration are added. The source and sink correspond to the viscous heating and inelastic dissipation terms, respectively, in the latter equation, the dilute-limit form of which in the JR theory for a system of rigid disks of diameter a whose collisions are characterized by a constant restitution coefficient $\tilde{e}$ is given by

$$\partial_t(\rho T) + \partial_\alpha(\rho u_\alpha T)$$

$$= \partial_\beta(\chi \partial_\beta T) - \rho T \partial_\beta v_\beta + \frac{1}{2}\eta \operatorname{Tr} \hat{D}^2_{\alpha\beta} - \frac{\rho^2}{\eta}(1 - \tilde{e}^2) T^2 \qquad (3)$$

where T is the granular temperature and ρ is the local solid fraction, i.e., fraction of volume of fluid occupied by the particles, which, apart for a multiplicative constant, is essentially the mass density. The thermal diffusivity χ and viscosity η are given by

$$\chi = 4\eta = \frac{\pi}{2}\sigma\sqrt{T} \qquad (4)$$

The dissipative term due to the inelasticity appears as the last term on the r.h.s of (3), and the viscous heating function is

$$\operatorname{Tr} \hat{D}^2_{\alpha\beta} = (\partial_\alpha v_\beta)^2 + (\partial_\alpha v_\beta \partial_\beta v_\alpha) - (\partial_\gamma v_\gamma)^2 \qquad (5)$$

Following the development in ref. 29, we define the mass density ρ by

$$\rho(\mathbf{x}, t) = \sum_{p, i} N_{pi}(\mathbf{x}, t) \qquad (6)$$

and the hydrodynamic velocity u_α by

$$\rho u_\alpha = \sum_{p, i} N_{pi} c_{pi\alpha} \qquad (7)$$

We introduce the quantity

$$\rho_1 = \sum_{p, i} N_{1pi} \qquad (8)$$

which may be thought of as the mass density of a component species whose particle density is N_{1pi}. The dependence of N_{pi}, N_{1pi}, u_α, and ρ_1 on x and t is implied for notational convenience and will be implied henceforth. The variable corresponding to the granular temperature is defined as

$$T = \frac{\rho_1}{\rho} \qquad (9)$$

where it is noted that, unlike the case of a true concentration variable, no constraint will be placed on the magnitude of ρ_1 relative to ρ and thus T may take all values larger than zero.

The evolution equation for N_{pi} is taken to be (1) with a forcing term added to its r.h.s. to recover the dependence of the pressure on T, i.e.,

$$N_{pi}(\mathbf{x} + \mathbf{c}_{pi}, t + 1) = N_{pi}(\mathbf{x}, t) - w[N_{pi}(\mathbf{x}, t) - N_{pi}^c(\mathbf{x}, t)]$$

$$+ \frac{t_p}{c_s^2} [\rho c_{pi\alpha} \partial_\alpha T + (T - c_s^2) c_{pi\alpha} \partial_\alpha \rho] \qquad (10)$$

The various derivatives in the forcing term depend only on the local state of the fluid at time t and can be computed using appropriate finite-difference approximations. The evolution equation for N_{1pi} is

$$N_{1pi}(x_\alpha + c_{pi\alpha}, t + 1)$$

$$= N_{1pi}(x_\alpha, t) - w_1[N_{1pi}(x_\alpha, t) - N_{1pi}^c(x_\alpha, t)]$$

$$+ t_p \left(\frac{1}{2} \eta \, \mathrm{Tr} \, \hat{D}^2 - \frac{\rho^2(1 - \tilde{e}^2) T^2}{\eta} \right) \qquad (11)$$

where η has already been defined in (4), $N_{1pi}^c \equiv T N_{pi}^c$, and a relaxation parameter w_1 possibly different from w may be used. On the macroscopic

scale, the dynamics of N_{1pi} and N_{pi} reproduce the dynamics of the granular temperature equation and those of the momentum and continuity equations, respectively. Thus, by coupling N_{1pi} to N_{pi} via u_α, a convective-diffusive effect on T is produced. The last two terms on the r.h.s of (11) correspond to a source and sink of temperature and, as in the case of the forcing term in (10), may be computed using finite difference approximations. To obtain the requisite dependence of η and χ on T [cf. (4)], the values of ψ and ψ_1 are coupled to the local value of T as follows:

$$\eta = \frac{c_s^2}{2}\left(\frac{2}{\psi}-1\right) = \frac{\sqrt{\pi}}{8}\sigma\sqrt{T} \qquad (12)$$

$$\chi = \frac{c_s^2}{2}\left(\frac{2}{\psi_1}-1\right) = \frac{\sqrt{\pi}}{2}\sigma\sqrt{T} \qquad (13)$$

Since ψ and ψ_1 are now regarded as functions of T, the only adjustable external parameters of this LBGK model are $\tilde{e}$ and σ, where $0 < \tilde{e} < 1$, and σ should be given in units of the lattice constant.

The macrodynamical equations for this model can be obtained by means of a Chapman–Enskog procedure, the complete details of which can be found in refs. 26 and 29. It can be shown finally that the macrodynamical equations for this model are

$$\partial_t \rho + \partial_\alpha(\rho u_\alpha) = 0 \qquad (14)$$

$$\partial_t(\rho u_\alpha) + \partial_\beta(\rho u_\alpha u_\beta) = -\partial_\alpha(\rho T) + \partial_\beta[\eta\partial_\beta(\rho u_\alpha) + \eta\partial_\alpha(\rho u_\beta)] \qquad (15)$$

$$\partial_t(\rho T) + \partial_\alpha(\rho u_\alpha T) = \partial_\alpha(\chi\rho\partial_\alpha T) + \frac{1}{2}\eta\operatorname{Tr}\hat{D}^2 - \frac{\rho^{2\tilde{e}T}}{\eta}2 \qquad (16)$$

Except for the absence in (16) of the term $\rho T\partial_\alpha v_\alpha$ (expansion work done by pressure), (12)–(16) correspond exactly to the JR equations. The key points of the Chapman–Enskog procedure relevant to the derivation of (14)–(16) are given in the appendix.

3. NUMERICAL RESULTS

The model described in the previous section is now used to compute solutions of the JR equations for the following flow configurations: an unforced granular gas in a periodic square domain whose temperature and density are initially homogeneous, and a Couette flow in a square domain which is bounded by two walls moving in opposite directions and which is periodic in the streamwise direction. The model is implemented on a 64×64 D2Q9 lattice with one rest and eight moving particles (cf. ref. 27 for

explanation of the D2Q9 lattice structure). In both configurations, the initial temperature field is uniform, while a 1% random perturbation is added to the initial density field, whose average is uniform, in order to trigger the nonlinear mechanism that leads to clustering. In the Couette flow, a uniform shear is also superposed and a no-slip condition is applied at the walls. This condition is maintained by specularly reflecting particles off them and by constraining u_α to the value of the wall velocity when computing the equilibrium particle density N_{pi}^e at nodes lining the walls.

The density and temperature fields for an unforced flow with $\bar{e} = 0.6$ and $\sigma = 0.05$ (where the lattice spacing is unity) at time $t = 100$ are shown in Figs. 1 and 2, respectively. These figures indicate that regions of higher density, corresponding to clusters, have lower temperatures, while regions of lower density have higher temperatures. The appearance of a characteristic length scale ion the density field is also evident in its Fourier transform, which shows an extremely well-defined peak at a single wavenumber. Solutions for other values of $\bar{e}$ show that this length scale decreases with increasing $\bar{e}$, in conformity with a theory for cluster creation based on the JR equations proposed in ref. 11. The fluctuations in the density and
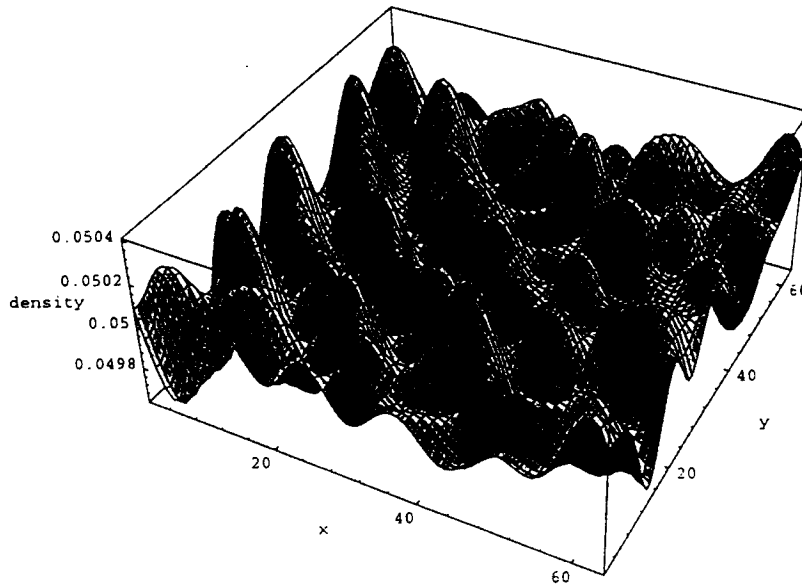

Fig. 1. Contour plot of the mass density field at $t = 300$ for a two-dimensional unforced flow governed by the JR equations with $\bar{e} = 0.6$ and $\sigma = 0.05$. The solution for the flow is computed using the LBGK model as presented in the text. The vertical axis corresponds to the local solid fraction (or dimensionless density) ρ in arbitrary units.

temperature fields can be as large as 20% of the corresponding average values. However, the dynamics for $t \gg 100$ shows that the density field saturates at the approximately same level of fluctuations as shown in Fig. 1. In contrast, molecular dynamics simulations of large unforced systems with the same value of $\bar{e}$ have shown that the density in the clusters could grow to several times the average density.[10] It thus appears that the JR equations, while faithful to the dynamics of the flow in the initial cluster-forming stage, do not capture its long-time dynamics. Moreover, the results for Couette flow presented below indicate that the anisotropic structure of the density inhomogeneities (i.e., the clusters) is not reproduced by these equations. This anisotropic structure has been observed in numerical simulations of periodic shear flows of frictionless disks and spheres ("Lees–Edwards" systems) and wall-bounded shear flows of both frictional and frictionless disks.[32] These simulations suggest that the structure of the density field in the interior of the flow is determined by the rotating and stretching effects of the shear in conjunction with a complex cluster–cluster scattering mechanism (explained in ref. 32) and is independent of the precise nature of the shearing boundary condition. The presence of rigid
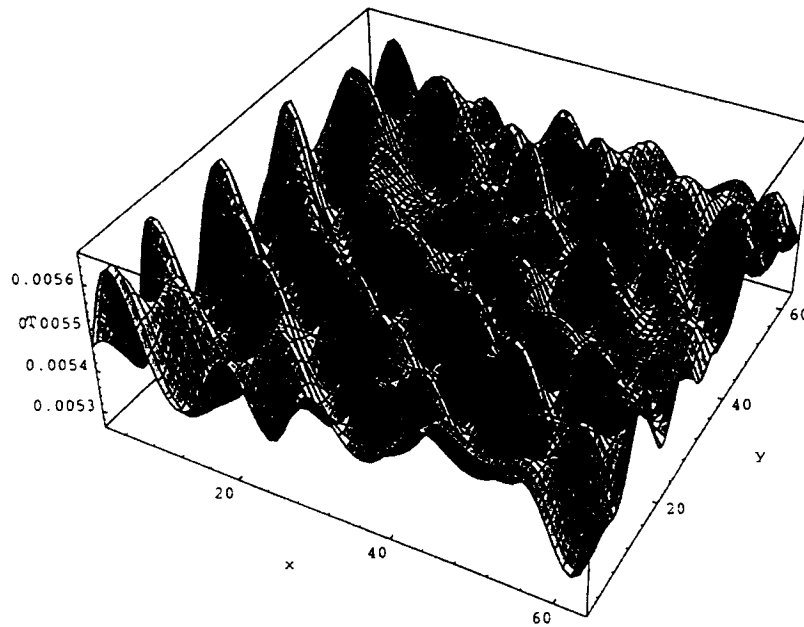

Fig. 2. Contour plot of the corresponding granular temperature field for the same unforced flow as shown in Fig. 1. The initial value of the granular temperature is set to unity.

moving walls additionally imposes a flow-scale inhomogeneity on the smaller scale anisotropic structure of the clusters, but the anisotropy remains nonetheless.

The density field for a Couette flow with $\bar{e} = 0.6$, $\sigma = 0.05$, and wall velocity $U = \pm 0.1$ (where the average particle speed c_s is $1/\sqrt{3}$) at $t = 100$ is shown in Fig. 4. Again a characteristic length scale can be seen, but the density inhomogeneities are isotropic, in contrast to the results of molecular dynamics simulations[32] (cf. Fig. 3), which show that dense clusters are created in the 45 deg direction, then are rotated by the shear before being broken up by their mutual interactions, and thus persist in the
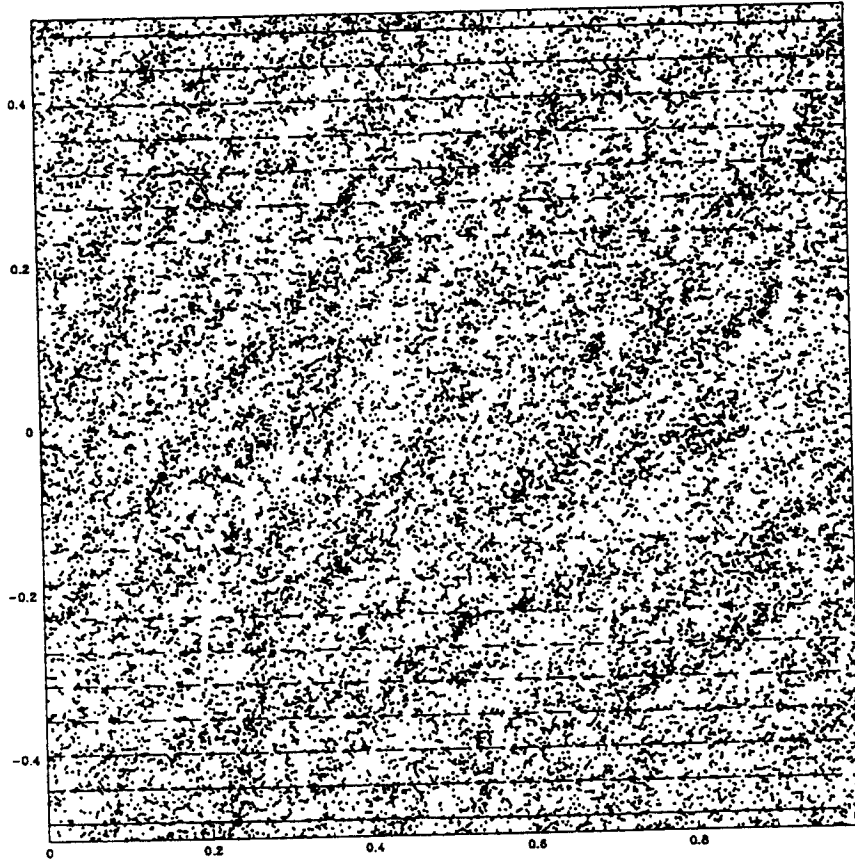

Fig. 3. The particle configuration plot for a two-dimensional simple shear flow of rigid inelastic disks whose restitution coefficient $\bar{e}$ is equal to 0.6. Superposed on the plot is a vector plot of the velocity field. The flow as shown is in a statistically steady state and is computed using a molecular dynamics program. The number of disks in the system is 2×10^5 and the volume fraction of the disks is 0.05.

flow only at angles of inclination between 0 and 45 deg to the horizontal, with the majority inclined at angles close to 45 deg.[32] It is also known that the second tensor moment of the velocity fluctuations is anisotropic in a shear flow[34] (i.e., that the normal kinetic stresses are different), but the JR theory assumes a vanishing normal stress difference. The solution for a transient period near $t = 0$ shows that the density fluctuations grow slightly, but the solution after long times indicates that both the density and temperature fluctuations decay and are eventually completely damped out. The state that is reached finally is a steady uniform shear flow with no inhomogeneities in either the density or the temperature field. Other solutions that were computed for different parameter values and from more strongly perturbed initial states behave in the same way after long times as well. It is not clear at this point whether the absence of clustering in the
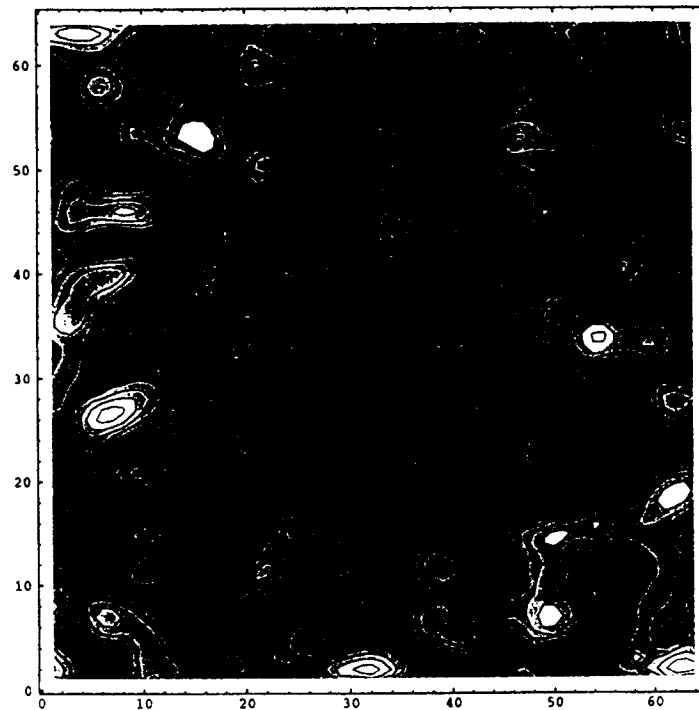

Fig. 4. Contour plot of the density field at $t = 100$ for a two-dimensional Couette flow governed by the JR equations with $\bar{e} = 0.6$ and $\sigma = 0.05$. The horizontal direction is the streamwise direction and the shade code for the plot is lighter shades for higher densities and darker shades for lower densities. Notice that the density inhomogeneities do not appear to lie in any preferred direction, in contrast to the molecular dynamics result shown in Fig. 1, which shows that the actual inhomogeneities are aligned typically at 45 deg from the horizontal.

long-time dynamics of the flow is an inherent property of the JR equations (i.e., that their shear flow solution is stable to finite-amplitude perturbations) or is due to an overdamping mechanism in the LBGK model itself. The LBGK model may be unsuitable for highly compressible flows, since the macrodynamical equations in the form shown in (14)–(16) are valid only in the limit of small Knudsen and small Mach numbers. It remains to be seen in future work whether the above findings can be borne out by simulations of the JR equations using other methods.

4. CONCLUSION

In this paper, we have constructed an LBGK model for a set of continuum equations for dilute two-dimensional granular flow and shown that they reproduce the phenomenon of clustering in unforced flows. However, they fail to reproduce the anisotropic cluster structures that are observed in molecular dynamics simulations of sheat flows, and their long-time solutions for these flows are homogeneous, also in contrast to the molecular dynamics results. The choice of the LBGK method, as opposed to more conventional methods such as finite-difference schemes, is made mainly on the basis of its algorithmic simplicity and adaptability to different rheological models, and also the ease with which the transport coefficients can be tuned or coupled to the field variables.

APPENDIX. CHAPMAN–ENSKOG EXPANSION OF THE LBGK EQUATION

We first derive the macrodynamical equations for a miscible multicomponent fluid modeled by the LBGK equation. Then we will show that by adding a suitable forcing term to (1) we may obtain an equation governing the dynamics of the concentration variable which is similar in form to the equation for the granular temperature. We first extend the definitions of the mass and momentum densities for a simple fluid to a mixture of fluids.[4] Let N_{rpi} denote the average population of particles of the rth species with velocity $c_{pi\alpha}$. The total mass density ρ is given by

$$\rho = \sum_{r,\,p,\,i} N_{rpi}(\mathbf{x},\,t) \tag{A1}$$

while the mass density ρ_r of the rth species is

$$\rho_r = \sum_{p,\,i} N_{rpi} \tag{A2}$$

Note that the sum is not taken over r in (A2). Also, the space and time dependence of N_{rpi} in (A2) is implied, and will be implied henceforth in the analysis. The velocity u_α in a mixture of fluids is defined as the total momentum of unit mass of fluid. That is, it is defined via the relation

$$\rho u_\alpha = \sum_{r, p, i} N_{rpi} c_{pi\alpha} \qquad (A3)$$

The additional hydrodynamic variables relevant to a mixture are those that describe the local composition of the fluid. These are the concentration c_r of the rth species and are defined as

$$c_r = \frac{\rho_r}{\rho} \qquad (A4)$$

In a mixture consisting of nonreacting species, the local concentration of each species changes through the mechanical mixing of the fluid and through mutual diffusion. From the definition (20), the c_r satisfy

$$\sum_r c_r = 1 \qquad (A5)$$

Hence for a mixture having a total of R species, there will be $(R-1)$ independent equations of motion for the c_r.

The generalization of (1) to a mixture of fluids is taken to be

$$N_{rpi}(x_\alpha + c_{pi\alpha}, t+1)$$
$$= N_{rpi}(x_\alpha, t) - w_r [N_{rpi}(x_\alpha, t) - N^e_{rpi}(x_\alpha, t)] \qquad (A6)$$

where possibly different relaxation parameters w_r may be assigned to each species. The local equilibrium population N^e_{rpi} can be inferred from a generalization of the H-theorem for a mixture of fluids and is given by

$$N^e_{rpi} = c_r N^e_{pi} \qquad (A7)$$

with N^e_{pi} given by (2). Equation (A7) may be taken to imply that the dynamics are attracted to separate equilibrium states corresponding to each component, but which are coupled via the velocity u_α.

The equations governing the large-scale dynamics of (A6), in which the local equilibrium distribution N^e_{rpi} is taken to be given by (A7), will now be derived using a Chapman–Enskog expansion. Since similar expansions for the LGA and LBE have been used before (see, for example, refs.

6 and 7), we will only outline here the steps necessary to obtain expressions for the transport coefficients. We assume a weak disequilibrium expansion

$$N_{rpi} = N_{rpi}^e + \varepsilon N_{rpi}^{(1)} + \varepsilon^2 N_{rpi}^{(2)} + \cdots \tag{A8}$$

where ε is the appropriate Knudsen number for the flow. The space and time derivatives are expressed in terms of multiple-scale variables as

$$\partial_\alpha = \varepsilon \partial_\alpha \tag{A9}$$

$$\partial_t = \varepsilon \partial_{t_1} + \varepsilon^2 \partial_{t_2} \tag{A10}$$

Since mass and momentum are conserved, it follows from (A6) and (A8) that

$$\sum_{r, p, i} w_r N_{rpi}^{(j)} = 0, \qquad j > 0 \tag{A11}$$

$$\sum_{r, p, i} w_r N_{rpi}^{(j)} c_{pi\alpha} = 0, \qquad j > 0 \tag{A12}$$

Also implicit in the lattice-BGK model is that the nonequilibrium populations $N_{rpi}^{(j)}$, $j > 0$, satisfy the constraints

$$\sum_{r, p, i} N_{rpi}^{(j)} = 0, \qquad j > 0 \tag{A13}$$

$$\sum_{r, p, i} N_{rpi}^{(j)} c_{pi\alpha} = 0, \qquad j > 0 \tag{A14}$$

$$\sum_{p, i} N_{rpi}^{(j)} = 0, \qquad j > 0 \tag{A15}$$

where (A15) expresses the conservation of the mass density of each species. However, $\sum_{p, i} N_{rpi}^{(j)} c_{pi\alpha}$ does not vanish in general, since there can be transfer of momentum from the particles of one species to particles of a different species.

By expanding N_{rpi} in a Taylor series about x_α and t, and using (A9) and (A10), we obtain first- and second-order equations in ε; we then take the zeroth and first moments of c_{pi} in these equations to obtain

$$\partial_{t_1} \rho + \partial_\alpha (\rho u_\alpha) = 0 \tag{A16}$$

$$\partial_{t_1} (\rho u_\alpha) + \partial_\beta J_{\alpha\beta} = 0 \tag{A17}$$

where it can be shown by using the fact that

$$\sum_p t_p \sum_{i=1}^{b_p} c_{pi\alpha} c_{pi\beta} c_{pi\gamma} c_{pi\delta} = c_s^4 (\delta_{\alpha\beta} \delta_{\gamma\delta} + \delta_{\delta\beta} \delta_{\gamma\alpha} + \delta_{\gamma\beta} \delta_{\alpha\delta}) \tag{A18}$$

that

$$J_{\alpha\beta} = c_s^2 \rho \delta_{\alpha\beta} + \rho u_\alpha u_\beta \tag{A19}$$

Using (A11), (A12), (A16), and (A17), we also obtain

$$\partial_{t_2} \rho = 0 \tag{A20}$$

$$\partial_{t_2} \rho u_\alpha + \partial_\beta \sum_{r,p,i} \left(1 - \frac{w_r}{2}\right) N_{rpi}^{(1)} c_{pi\alpha} c_{pi\beta} = 0 \tag{A21}$$

Equation (A20) implies that there is no diffusion of the total mass density, while (A21) accounts for the effect of viscous momentum fluxes.

Following the development of the Chapman–Enskog expansion, $N_{rpi}^{(1)}$ will now be expressed in terms of derivatives of the macroscopic variables. Here we will also need equations corresponding to (A16) and (A17) in which the index r is not summed over. These are

$$\partial_{t_1} \rho_r + \partial_\alpha(\rho_r u_\alpha) = 0 \tag{A22}$$

$$\partial_{t_1}(\rho_r u_\alpha) + c_s^2 \partial_\alpha \rho_r + \partial_\beta(\rho_r u_\alpha u_\beta) = -w_r \sum_{p,i} N_{rpi}^{(1)} c_{pi\alpha} \tag{A23}$$

Note that $\sum_{p,i} N_{rpi}^{(1)} c_{pi\alpha}$ corresponds to the nonequilibrium mass flux of species r and does not vanish in general. To $\mathcal{O}(u)$ this flux is given by

$$\sum_{p,i} N_{rpi}^{(1)} c_{pi\alpha} = -\frac{1}{w_r} [\partial_{t_1}(\rho_r u_\alpha) + c_s^2 \partial_\alpha \rho_r] + \mathcal{O}(u^2) \tag{A24}$$

It is easy to show using (A17), (A19), and the relation $\rho_r = \rho c_r$ that $\partial_{t_1}(\rho c_r u_\alpha) = -c_s^2 c_r \partial_\alpha \rho + \mathcal{O}(u^2)$. Hence

$$\sum_{p,i} N_{rpi}^{(1)} c_{pi\alpha} = \frac{-c_s^2}{w_r} \rho \partial_\alpha c_r + \mathcal{O}(u^2) \tag{A25}$$

Using (A7), (A22), and (A23), we obtain finally

$$N_{rpi}^{(1)} = -\frac{t_p}{w_r} \left[\left(\frac{c_{pi\alpha} c_{pi\beta}}{c_s^2} - \delta_{\alpha\beta} \right) \partial_\beta(\rho_r u_\alpha) + c_{pi\alpha} \rho \hat{c}_\alpha c_r \right] \tag{A26}$$

It is easy to check that the conditions (A13)–(A15) are satisfied by $N_{rpi}^{(1)}$. Substituting (A26) into (A21), we obtain finally

$$\partial_{t_2}(\rho u_\alpha) - \partial_\beta \left\{ \frac{c_s^2}{2} \left(\frac{2}{w} - 1 \right) [\partial_\alpha(\rho u_\beta) + \partial_\beta(\rho u_\alpha)] \right\} = 0 \tag{A27}$$

where we have defined the "equivalent" relaxation parameter w via the relation

$$\frac{1}{w} = \sum_r \frac{c_r}{w_r} \tag{A28}$$

Equations (A16), (A17), (A20), and (A27), i.e. the dynamical equations from the two separated time scales $1/\varepsilon$ and $1/\varepsilon^2$, will now be reconstituted to obtain the macrodynamical equations for the model. The equation of continuity is obtained from (A16) and (A20) by multiplying the former by ε and the latter by ε^2 and then adding the two equations; and the Navier–Stokes equation is obtained from (A17) and (A27) in the same manner. We obtain

$$\partial_t \rho + \partial_\alpha(\rho u_\alpha) = 0 \tag{A29}$$

$$\partial_t(\rho u_\alpha) + \partial_\beta(\rho u_\alpha u_\beta) = -c_s^2 \partial_\alpha \rho + \partial_\beta[\nu \partial_\beta(\rho u_\beta) + \zeta \partial_\alpha(\rho u_\beta)] \tag{A30}$$

where the coefficients of shear viscosity ν and bulk viscosity ζ are given by

$$\nu = \zeta = \frac{c_s^2}{2}\left(\frac{2}{w} - 1\right) \tag{A31}$$

We will now obtain the equation of motion for the concentration c_r. The equation corresponding to (A20) in which indices p and i are not summed over is

$$\partial_{t_2}\rho_r - \left(\frac{w_r}{2} - 1\right)\partial_\alpha\left(\sum_{p,\,i} N_{rpi}^{(1)} c_{pi\alpha}\right) = 0 \tag{A32}$$

which shows that there in general the species mass densities change on the diffusive time scale. Substituting (A25) into (A32), we obtain, correct to $\mathcal{O}(u)$, the convective-diffusive equations for the mass density of each species

$$\partial_t(\rho c_r) + \partial_\alpha(\rho c_r u_\alpha) = \partial_\alpha(D_r \rho \partial_\alpha c_r) \tag{A33}$$

where the diffusivity is given by

$$D_r = \frac{c_s^2}{2}\left(\frac{2}{w_r} - 1\right) \tag{A34}$$

For a mixture of two species with $\rho_1 = \rho_2$ and $w_1 = w_2$, we find that $D_1 = D_2 = \nu$. This is not surprising, since the concentration variable is analogous to the temperature in the BGK approximation and the Prandtl number (ratio of viscosity to temperature diffusivity) of a gas that satisfies

the BGK equation is unity. Also, notice that since $\sum_{p,i} N^{(1)}_{rpi} c_{pi\alpha}$ does not vanish in general, (A12) implies that all but one of the w_r are freely adjustable. Thus in practice one prescribes values for the equivalent relaxation parameter w and w_r, $r = 1, 2,..., R - 1$ (where R is the total number of species), and uses Eq. (A6) for N_{rpi}, $r = 1, 2,..., R - 1$, together with an additional equation for the total population $N_{pi} \equiv \sum_{r,p,i} N_{rpi}$ [which is exactly similar in form to (1) with the corresponding N^e_{pi} given by (2)] to compute the evolution of the dynamics.

Equations (12)–(16) are obtained as a straightforward extension of the above model. We consider a two-component fluid and define

$$T = c_1 = \frac{\rho_1}{\rho} \tag{A35}$$

The continuity equation (14) is derived in exactly the same way as (A29). It is easy to see that the last term on the r.h.s. of (10), when summed over p, produces a term that cancels the pressure term in (A29) and replaces it with $-\partial_\alpha(\rho T)$. The last term on the r.h.s. of (11), when summed over p, produces an equation for ρ_1 given by

$$\partial_{t_2}\rho_r - \left(\frac{w_r}{2} - 1\right)\partial_\alpha\left(\sum_{p,i} N^{(1)}_{rpi} c_{pi\alpha}\right) + \left(\frac{1}{2}\eta \, \text{Tr} \, \hat{D}^2 - \frac{\rho^2(1 - \bar{e}^2)T^2}{\eta}\right) = 0 \tag{A36}$$

from which (16) follows with ξ equal to D_1 as given by (A34).

REFERENCES

1. P. Bhatnagar, E. P. Gross, and M. K. Krook, *Phys. Rev.* 94:511 (1954).
2. C. S. Campbell, *J. Fluid Mech.* 203:449–473 (1989).
3. C. S. Campbell and C. E. Brennan, *Trans. ASME: J. Appl. Mech.* 52:172–178 (1985).
4. S. Chapman and T. G. Cowling, *The Mathematical Theory of Nonuniform Gases.* 3rd ed. (Cambridge University Press, Cambridge, 1970).
5. D. d'Humières, P. Lallemand, and U. Frisch, *Europhys. Lett.* 2:291 (1980).
6. G. D. Doolen, ed., *Lattice Gas Methods for Partial Differential Equations* (Addison-Wesley, Reading, Massachusetts, 1990).
7. U. Frisch, D. d'Humières, B. Hasslacher, P. Lallemand, Y. Pomeau, and J.-P. Rivet, *Complex Systems* 1:649 (1987).
8. U. Frisch, B. Hasslacher, and Y. Pomeau, *Phys. Rev. Lett.* 56:1505 (1986).
9. I. Goldhirsch, M.-L. Tan, and G. Zanetti, *J. Sci. Comp.* 8(1):1 (1993).
10. I. Goldhirsch and G. Zanetti, *Phys. Rev. Lett.* 70:1619–1662 (1993).
11. P. K. Haff, *J. Fluid Mech.* 134:401–430 (1983).
12. H. J. Herrmann, *Physica A* 191:263–276 (1992).
13. M. A. Hopkins and M. Y. Louge, *Phys. Fluids A* 3(1):47–57 (1991).
14. J. T. Jenkins and M. W. Richman, *Arch. Rat. Mech. Anal* 87:355–377 (1985).
15. J. T. Jenkins and M. W. Richman, *Phys. Fluids* 28:3485–3494 (1985).
16. J. T. Jenkins and M. W. Richman, *Phys. Fluids* 28:3485–3494 (1985).

17. J. T. Jenkins and S. B. Savage, *J. Fluid Mech.* **130**:187–202 (1983), and references therein.
18. C. K. K. Lun, *J. Fluid Mech.* **223**:539–559 (1991).
19. C. K. K. Lun and S. B. Savage, *J. Appl. Mech.* **154**:47–53 (1987), and references therein.
20. S. McNamara, *Phys. Fluids A* **5**:3056–3070 (1993).
21. S. McNamara and W. R. Young, *Phys. Fluids A* **4**:496–504 (1992).
22. S. McNamara and W. R. Young, *Phys. Fluids A* **5**:34–45 (1993).
23. S. Ogawa (Gukujutsu Bunken Fukyukai, Tokyo, 1978),Vol. 31, pp. 208–217.
24. T. Pöschel, *J. Phys. II France* **3**:27–40 (1993).
25. Y. H. Qian, Lattice Gas and lattice kinetic theory applied to Navier-Stokes equation, Ph.D. thesis, University of Paris 6 (1990).
26. Y. H. Qian, D. d'Humières, and P. Lallemand, *Europhys. Lett.* **17**(6):479–484, (1992).
27. Y. H. Qian and S. A. Orszag, *Europhys. Lett.* **21**(3):255–259 (1993).
28. Y. H. Qian, M.-L. Tan, and S. A. Orszag, A lattice-BGK model for miscible fluids, in *Proceedings 5th International Symposium on Computational Fluid Dynamics* (Sendai, Japan, 1993).
29. S. B. Savage, *J. Fluid Mech.* **241**:109–123 (1992).
30. P. J. Schmid and H. K. Kytomaa, *J. Fluid Mech.* **264**:255–275 (1994).
31. M.-L. Tan, Microstructures and macrostructures in rapid granular flows, Ph.D. thesis, Princeton University, (1995).
32. O. R. Walton, H. Kim, and A. D. Rosato (ASCE, New York, 1991), Vol. 2, pp. 1249–1253.